

# Surface oxidation of Al masks for deep dry-etch of silica optical waveguides

Wei-Tang Li<sup>\*</sup>, D.A.P. Bulla, Rod Boswell

*Plasma Research Laboratory, Research School of Physical Sciences and Engineering, The Australian National University, ACT 0200, Australia*

Available online 4 August 2006

## Abstract

The surface oxidation of Al metal masks in an oxygen plasma was studied for realizing deep dry-etch of silica optical waveguides. The oxidation efficiency of the plasma was found to depend on mainly substrate bias and plasma power. Net sputtering effect happened when ion bombarding potential exceeds certain critical value. However, suitable ion bombarding energy is of benefit to the oxidation process. There was a saturation thickness of the Al<sub>2</sub>O<sub>3</sub> layer, beyond which the growth rate of Al<sub>2</sub>O<sub>3</sub> films became very low. The saturation thickness increased with the plasma power. According to these growth characteristics, the oxide growth mechanisms were discussed, and suitable plasma conditions were chosen for the surface oxidation of Al metal masks. Under the chosen plasma conditions, a thick Al<sub>2</sub>O<sub>3</sub> layer of ~6.5 nm was generated in a short time of 2 min. Thus the surface of the Al metal mask could be periodically oxidized during the breaks of the silica etching process to enable much higher SiO<sub>2</sub>/mask etching selectivity of ~100:1, in comparison with ~15/1 obtained without the surface oxidation process. This greatly reduced the required Al mask thickness from over 500 to 100 nm for a deep silica etch of over 5 μm, and led to the achievement of high-quality silica waveguides with vertical and very smooth sidewalls.

© 2006 Elsevier B.V. All rights reserved.

PACS: 52.77; 52.40; 81.15; 81.65; 82.45

Keywords: Plasma oxidation; plasma etching; Al<sub>2</sub>O<sub>3</sub> mask; Silica optical waveguides; Sidewall roughness

## 1. Introduction

Deep dry-etch of silica (~5–10 μm thick) is the key step in the fabrication process of the silica-based channel waveguides, which are the most potential building blocks of planar lightwave circuits for future optical telecommunication systems [1–5]. It is required that the etched waveguides possess vertical sidewalls for accurate dimension control, and the sidewalls need to be very smooth for avoiding surface roughness induced scattering loss of the guiding lights. To realize vertical and smooth sidewalls of a thick waveguide is however not easy, since a thick etching mask is normally required, and the mask fabrication processes (lithograph and etching) always induce certain roughness and slope to the sidewalls of the mask patterns, which are transferred to the underlying silica layer during the silica-etch process. The thicker the mask layer, the higher roughness and the greater slope could be generated in the mask patterns during the mask fabrication processes. Reducing the mask thickness is therefore essential for effectively reducing the

process-induced defects to the masks. This requires increasing the silica etching selectivity over the mask.

Instead of the conventional masking materials, such as Cr [1,2], amorphous silicon [3], photoresist [4], and Al [5], Al<sub>2</sub>O<sub>3</sub> thin films were chosen as the masking materials in this work. To simplify the Al<sub>2</sub>O<sub>3</sub> mask fabrication process, an Al metal mask was fabricated first, and then its surface was oxidized periodically in an O<sub>2</sub>-plasma during the breaks of the silica-etch process in a helicon plasma reactor. The Al<sub>2</sub>O<sub>3</sub> layer was found to offer an extremely high SiO<sub>2</sub>/Al<sub>2</sub>O<sub>3</sub> etching selectivity of ~100:1 in a CF<sub>4</sub> plasma, which was much higher than the SiO<sub>2</sub>/Al selectivity of ~15:1 or the SiO<sub>2</sub>/Cr selectivity of ~27/1, at the same plasma condition. Thus a very thin Al<sub>2</sub>O<sub>3</sub> mask (70–100 nm), rather than a thick Al (>500 nm) or Cr mask (>200 nm), was enough for etching over a 5-μm-thick SiO<sub>2</sub>. Such a reduction of the mask thickness greatly reduced the fabrication processes induced roughness to the mask, and provided the possibility to accurately control the line width of the masks and the waveguides. In addition, the thin Al masks were very easy to be fabricated using lift-off or dry-etch techniques developed in the integrated circuit processing.

In order to efficiently oxidize the Al mask surface with O<sub>2</sub> plasma in the helicon plasma etcher, the influences of different

<sup>\*</sup> Corresponding author. Tel.: +61 2 61252832; fax: +61 2 61250029.

E-mail address: [weitang.li@anu.edu.au](mailto:weitang.li@anu.edu.au) (W.-T. Li).

plasma parameters to the oxidation effect were investigated and optimized, so that a thick oxide layer can be produced in a very short time. The surface oxidation of Al using different techniques, such as electron irradiation [6,7], exposure to water vapor [8], exposure to ozone [9], thermal oxidation [10], and plasma treatment [11,12], has been reported. However, quick oxidation under high-density plasma is rarely reported, and is thus studied in this work.

## 2. Experiment procedure

### 2.1. Sample preparation

The silica thin films (5–7  $\mu\text{m}$  thick) to be etched were produced using a helicon plasma activated reactive evaporation technique [13]. The masking materials, metal Al and Cr films, are deposited on the silica films using a DC magnetron sputtering technique [14].

Thin Al masks of  $\sim 100$  nm thick were patterned using a lift-off process. For comparison, 500-nm-thick Al, and 300-nm-thick Cr metal masks were also fabricated on some silica samples using wet-etching processes. The etchants were  $\text{H}_3\text{PO}_4:\text{HNO}_3:\text{HAc}:\text{H}_2\text{O}=16:1:1:2$  for the Al, and  $\text{Ce}_2\text{SO}_4:\text{HNO}_3=9:1$  for the Cr.

Very thin ( $<20$  nm) Al films were also prepared for the purpose of in-situ study of their surface oxidation using an ellipsometry technique, since thicker ( $>30$  nm) Al films are not transparent to visible lights, and cannot be measured accurately using the ellipsometer. These Al films were sputter-coated on bare Si wafers with the same vacuum base pressure ( $5 \times 10^{-7}$  Torr), Ar plasma pressure (6 mTorr), and target self-bias voltage ( $-400$  V), so that they have the same purity, density and average grain size, which are possible parameters to influence the oxide growth kinetics.

In addition, pure  $\text{Al}_2\text{O}_3$  layers of  $\sim 20$  nm thickness were prepared on some bare silicon wafers using a reactive sputtering technique [14], for testing the net sputtering rate of the  $\text{Al}_2\text{O}_3$  by  $\text{O}_2$  plasma.

### 2.2. Plasma processing

The oxidation of the Al surface was carried out in a helicon plasma reactor, which is a low-pressure high-density plasma source, and has been detailed elsewhere [15,16]. Before the oxide growth, the native  $\text{Al}_2\text{O}_3$  ( $\sim 4$  nm thick) layer covering the Al thin film was removed using  $\text{CF}_4$ -plasma etching with the conditions of plasma power 1000 W, substrate bias  $-25$  V, gas pressure  $\sim 2$  mTorr. After 2 min of the etching, oxide growth was started immediately by changing the processing gas from  $\text{CF}_4$  to  $\text{O}_2$ . During the oxide growth, the substrate was positively biased using a DC voltage source, or negatively biased with a RF power source, or simply earthed, so that the effect of different substrate bias on the oxide growth could be investigated.

Dry-etch of the silica layers was performed using the same helicon plasma reactor. For the thick Al or Cr masked samples, the etching of the waveguide was performed continuously in a

$\text{CF}_4$ -plasma; but for the thin (100 nm) Al-masked samples, the etching was periodically intervened for oxidizing the surface of the Al mask in an oxygen-plasma. The etching duration ( $\sim 2$  min) of the silica was set to keep the etched  $\text{Al}_2\text{O}_3$  thickness to be less than the grown during each of the period from the  $\text{Al}_2\text{O}_3$ -growth to the silica-etch.

### 2.3. Measurements

The applied in-situ ellipsometer is a variable angle spectroscopic system. It measures the optical parameters between the wavelength of 400 to 750 nm in each scan, and can provide accurate thickness of a very thin film ( $>\sim 0.5$  nm thick).

The etch rates of the  $\text{SiO}_2$  and the masking materials (Cr, Al and  $\text{Al}_2\text{O}_3$ ) were measured both in-situ using the ellipsometer, and ex-situ using a surface profilometer. The micrographs of the waveguides and masks were taken using a field emission scanning electron microscopy (FESEM). The sidewall roughness of the waveguides was determined by measuring the average amplitude of the corrugations or ripples within a 2- $\mu\text{m}$  range on the sidewalls using the FESEM.

## 3. Results and discussions

### 3.1. Al oxide growth and mechanisms

The time dependent thickness variation of the  $\text{Al}_2\text{O}_3$  grown from the Al surface in the  $\text{O}_2$  plasma is plotted in Fig. 1. The applied plasma power was 0, 600 or 1000 W as marked on the curves in the figure; the substrate bias was 0 V, and  $\text{O}_2$  plasma pressure  $\sim 2$  mTorr for all the cases. As seen in Fig. 1, only a very thin ( $<1$  nm)  $\text{Al}_2\text{O}_3$  layer grew in the case without plasma; but a quick oxide growth was seen when the plasma was applied; and the higher the plasma power, the quicker the  $\text{Al}_2\text{O}_3$  growth; the thickness of the  $\text{Al}_2\text{O}_3$  became nearly saturated after

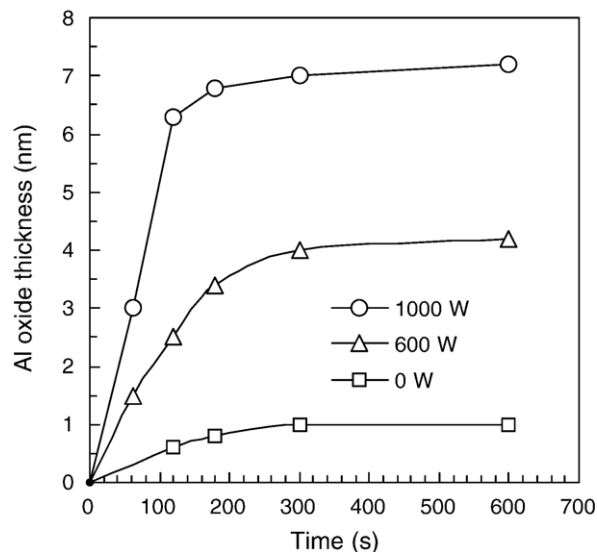


Fig. 1. Thickness of  $\text{Al}_2\text{O}_3$  grown on Al surface in the  $\text{O}_2$  plasma as a function of the plasma processing time. The substrate bias was 0 V, and the applied plasma power was as marked on the curves.

the initial quick growth period of  $\sim 300$  or  $180$  s for the  $600$  and  $1000$  W power, respectively; the saturation thickness of the  $\text{Al}_2\text{O}_3$  increased from  $\sim 4$  to  $7$  nm when increasing the plasma power from  $600$  to  $1000$  W. These indicate that the oxide growth efficiency is highly dependent on the plasma power, or on the plasma density, which is directly related to the plasma power.

In order to check the effect of substrate bias ( $V_b$ ) on the growth kinetics, the saturation thickness of the grown  $\text{Al}_2\text{O}_3$ , as well as the net sputtering rate of the  $\text{Al}_2\text{O}_3$ , were measured and plotted in Fig. 2. The applied plasma power was marked on the curves in the figure, and in all the cases, the  $\text{O}_2$  plasma pressure was  $\sim 2$  mTorr. As seen in Fig. 2, the net  $\text{Al}_2\text{O}_3$  sputtering rate under a plasma power of  $1000$  W was zero when the substrate was positively biased or earthed, but the sputtering began as long as a negative  $V_b$  was applied. The sputtering was observed even when the substrate was floated with a floating potential of  $V_f = -5$  V. This is due to the high plasma potential of the helicon reactor. With the above plasma conditions, the plasma potential was  $V_p \sim 20$  V, so that an ion bombardment potential equal to  $V_p - V_f = 25$  V was generated. This potential was enough for the  $\text{O}^+$  ions to cause sputtering on the surface of the Al or  $\text{Al}_2\text{O}_3$  material.

The saturation thickness ( $t_s$ ) of the grown  $\text{Al}_2\text{O}_3$ , is seen to be highly dependent on the substrate bias, as shown in Fig. 2. The maximum  $t_s$  seems to occur at around  $V_b = 0$  V;  $t_s$  decreases slightly with the increase of the positive  $V_b$ , due to, possibly, the fact that more and more  $\text{O}^+$  ions from the plasma were repelled by the substrate; the rapid decrease of  $t_s$  with the increase of negative bias should be attributed to the  $\text{O}^+$  sputtering effect. When the negative  $V_b$  is beyond certain critical value ( $V_{bc}$ ),  $t_s$  becomes negative, meaning that the  $\text{Al}_2\text{O}_3$  growth was fully suppressed by the sputtering process. The  $V_{bc}$  is  $\sim -20$  or  $-30$  V for the cases of  $1000$  and  $600$  W plasma power, respectively.

Different mechanisms have been proposed to explain the  $\text{Al}_2\text{O}_3$  growth kinetics under different environments [6–12]. We regard all the following mechanisms are involved in the surface oxidation of the Al films in the helicon plasma:

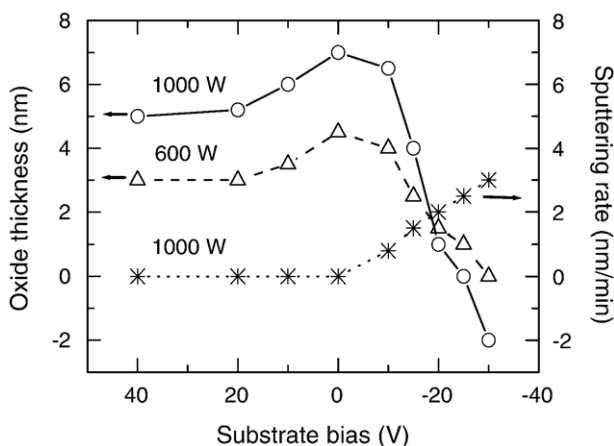


Fig. 2. Growth saturation thickness and net sputtering rate of the  $\text{Al}_2\text{O}_3$  films as functions of the substrate bias. The  $\text{O}_2$  plasma pressure was 2 mTorr, and plasma power  $600$  or  $1000$  W as marked on the curves.

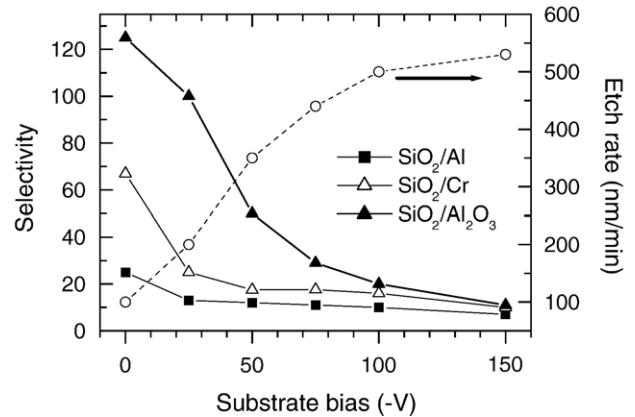


Fig. 3.  $\text{SiO}_2$  etching selectivities over  $\text{Al}_2\text{O}_3$ , Cr and Al, as well as the etch rate of  $\text{SiO}_2$ , versus the applied substrate bias  $V_b$ , when keeping plasma power  $1000$  W and  $\text{CF}_4$  gas pressure 2 mTorr.

### 3.1.1. Electron stimulated surface chemical reaction

Upon electron impact, electronically excited states of the reactant molecules are produced, leading to a quick chemical reaction between Al and  $\text{O}_2$ . The field of electron-stimulated films growth has been intensively studied for both metal and semiconductor surfaces [6,7]. In the helicon plasma reactor, a high electron density ( $\sim 10^{10}$ – $10^{11}$   $\text{cm}^{-3}$ ) is generated [16], the electrons are highly mobile, and they easily reach the substrate. In particular, when a positive bias was applied, more electrons were absorbed by the substrate, so that a thick  $\text{Al}_2\text{O}_3$  layer is still obtained even almost all of the  $\text{O}^+$  ions are repelled in the case of  $V_b > V_p$  ( $\sim 20$ – $30$  V), as indicated in Fig. 2.

### 3.1.2. Diffusion of Al ions

According to Cabrera–Mott theory [9,10], during the Al surface thermal oxidation, the electrons tunnel from the metal through the already formed oxide layer to absorb oxygen atom. The field set up by these trapped electrons reduces the activation energy for Al ions migration or hopping. Therefore it can pull ions from the Al metal layer through the oxide layer to meet the oxygen atoms. During the plasma oxidation, the electrons trapped on the  $\text{Al}_2\text{O}_3$  surface come not only from inside the Al layer, but also largely from the plasma. Thus a much stronger field can be built to pull the Al ions from inside the Al layer. Therefore the growth is much quicker than thermal oxidation. The diffusion of the Al ions is impeded or even stopped as the thickness of oxide layer increases. These could be some of the reasons for the observed growth characteristics shown in Fig. 1.

### 3.1.3. Ion sputtering and implantation

The oxygen ions coming from the plasma may remove the surface atoms of the films if the  $\text{O}^+$  have high enough energy. The minimum ion energy required to sputter the Al is very low, for example this energy is only 13 eV for Ar ion [17]. In particular, the helicon plasma reactor is a high-density plasma source with high plasma potential, thus the ion sputtering effect plays an important role in the surface oxidation process of the Al films. To reduce the ion sputtering effect, the sample needs to be earthed or positively biased, as indicated in Fig. 2. In

addition,  $O^+$  implantation into a shallow depth of the sample surface is also possible, since this effect is always accompanying the sputtering process [17].

#### 3.1.4. Diffusion of oxygen

Although Al ions are believed to be the dominant moving species during the Al surface oxidation process, oxygen transport through the boundary of Al grains to the inner Al region may also happen, as observed by Kuiper et al. [12], who used  $^{18}O_2$  to track the transport of O during the Al oxidation process.

#### 3.2. Silica etch rate and etching selectivity

Fig. 3 exhibits the variations of the  $SiO_2$  etch rates, as well as the  $SiO_2/Al_2O_3$ ,  $SiO_2/Al$  and  $SiO_2/Cr$  etching selectivities, versus  $V_b$  when keeping a  $CF_4$  gas pressure of 2 mTorr and

plasma power of 1000 W. As shown in Fig. 3, the etch rate of the silica, increases quickly with  $V_b$ , since the silica-etch is an ion bombardment dominated process. The total ion bombardment potential comes from both the  $V_b$  and the plasma potential of  $\sim 20$  V. Therefore, even at a low  $V_b$  of  $-20$  to  $-30$  V, a high ion bombardment energy of  $40$ – $50$  eV remained, and a high etch rate of around  $200$  nm/min for the silica was still achieved.

The  $SiO_2/Al_2O_3$  selectivity, as seen in Fig. 3, is much higher than that of the  $SiO_2/Al$  and  $SiO_2/Cr$  at low bias ( $<50$  V). For example, at  $V_b = -25$ , the silica etching selectivity over the  $Al_2O_3$ , Al and Cr are  $\sim 100$ , 27 and 15, respectively. This indicates that, at low substrate bias, the  $Al_2O_3$  is much more inert than the Al and Cr to the reactive species coming from the  $CF_4$  plasma. At higher bias ( $>50$  V), ion-sputtering effect may dominate for etching all the three masking materials, leading to the etching selectivities over them to decrease and even to draw close at a very high bias of over  $100$  V.

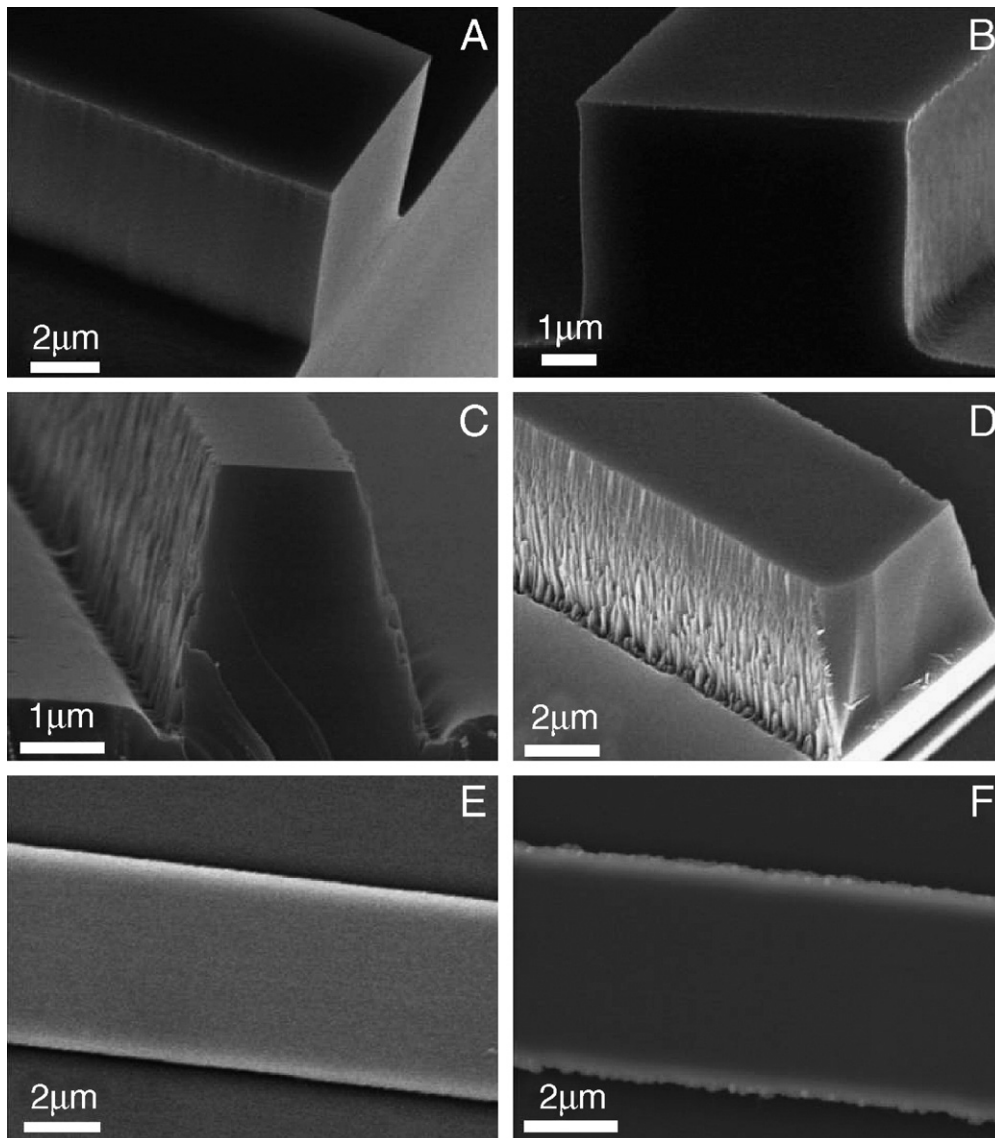


Fig. 4. A and B are the micrographs of the silica waveguides dry-etched under 100-nm-thick Al mask, whose surfaces were oxidized periodically during the etching process. C and D are the waveguides dry-etched under the wet-etched Al and Cr masks, respectively. E and F are the Al mask patterns fabricated using a lift-off and wet-etch technique, respectively.

Based on the experimental results showing in Fig. 3, we chose  $V_b = -25$  V for the SiO<sub>2</sub> etching, so that an extremely high SiO<sub>2</sub>/Al<sub>2</sub>O<sub>3</sub> etching selectivity of  $\sim 100:1$  was obtained, and a reasonably high SiO<sub>2</sub> etch rate of 200 nm/min was retained. For the Al mask surface oxidation, we chose the plasma conditions of power 1000 W, substrate bias 0 V, pressure of  $\sim 2$  mTorr. Thus we could set both the SiO<sub>2</sub>-etch and the Al<sub>2</sub>O<sub>3</sub>-growth durations to be 2 min, so that the etched Al<sub>2</sub>O<sub>3</sub> thickness ( $\sim 4$  nm) was less than the grown ( $\sim 6$  nm) during each of the period from the Al<sub>2</sub>O<sub>3</sub>-growth to the SiO<sub>2</sub>-etch. The plasma could be easily switched between the CF<sub>4</sub> and O<sub>2</sub> without the requirement of retuning the matching conditions of the plasma, since the applied power (1000 W), and the pressure ( $\sim 2$  mTorr) are the same during the SiO<sub>2</sub> etching and Al<sub>2</sub>O<sub>3</sub> growth.

### 3.3. Waveguide profiles

Fig. 4A and B illustrate the micrographs of two thick ( $>5$   $\mu\text{m}$ ) silica waveguides obtained using above special etching process. As seen here, high-quality waveguides with vertical and very smooth sidewalls were achieved. The average sidewall roughness of these waveguides was estimated to be  $\sim 10$  nm. Whereas, a waveguide with slanted and very rough sidewalls (roughness  $\sim 100$ – $150$  nm) was obtained, as shown in Fig. 4C, using the conventional plasma-etch process, in which a thick wet-etched Al mask was applied, and the surface of the mask was not oxidized periodically during the etching. The waveguides dry-etched under the wet-etched Cr masks also had slanted and very rough sidewalls, as shown in Fig. 4D. We found that the sidewall roughness and slope of the waveguides were mainly transferred from the etching masks, and the lower the etching selectivity, the greater slope of the mask was transferred to the waveguides. By employing the special etching process, very thin Al mask ( $\sim 100$  nm) is enough for etching the silica waveguide of over 5  $\mu\text{m}$  thick. Such a thin mask can be fabricated easily using a lift-off process to enable near vertical and very smooth sidewalls of the mask pattern, as shown in Fig. 4E. Otherwise, for the conventional etching process, a very thick ( $>500$  nm) Al mask is required. Such thick Al mask patterns with vertical and smooth sidewalls are very difficult to fabricate even using a dry-etching process. A wet-etch process is convenient for making the thick Al mask, but it normally generated very rough and slanted sidewalls of the mask patterns, as shown in Fig. 4F.

## 4. Conclusions

The influences of different plasma parameters to the Al surface oxidation were investigated. The ion bombarding energy and plasma density were found to be the critical parameters to determine the growth kinetics. Increasing the electron and ion densities by increasing the plasma power enhanced the plasma oxidation effect. Suitable ion bombarding energy is of benefit to the oxidation process but net sputtering happened when the ion bom-

barding potential exceeds certain critical value. At certain plasma power, there was a saturation thickness of the Al<sub>2</sub>O<sub>3</sub> layer, beyond which the growth rate of Al<sub>2</sub>O<sub>3</sub> films became very low. The saturation thickness increased with the plasma power. A thick Al<sub>2</sub>O<sub>3</sub> film ( $\sim 6.5$  nm) could be produced in 2 min under 1000 W plasma power and 0 V substrate bias, which was efficient enough for oxidizing the Al mask surface during the deep dry-etch of the silica waveguides.

Possible mechanisms involved in the Al surface oxidation are considered to be the electron stimulated surface chemical reaction, diffusion of Al ions, ion sputtering/implantation, and oxygen diffusion through the boundary of Al grains.

Based on the success of efficient Al surface oxidation, a novel and simple method for realizing vertical and very smooth sidewalls of the silica waveguides was developed. The Al<sub>2</sub>O<sub>3</sub> thin films grown from the Al surface were employed as the real mask layers for etching the waveguides. An extremely high SiO<sub>2</sub>/Al<sub>2</sub>O<sub>3</sub> etching selectivity of  $\sim 100:1$ , in contrast to a SiO<sub>2</sub>/Al selectivity of  $\sim 15:1$  at the same plasma conditions, was achieved. Such a high etching selectivity greatly reduced the required Al mask thickness from over 500 nm down to  $\sim 100$  nm, which made it easy to obtain high quality mask patterns, and enable the achievement of vertical and very smooth sidewalls of the silica waveguides.

## Acknowledgments

The support from Australia Research Council (ARC) through its discovery project program is acknowledged. The authors are also grateful to Dr. Cheng Huang in the Electronic Microscope Unit of ANU for giving assistance with the FESEM application.

## References

- [1] A.K. Dutta, Jpn. J. Appl. Phys. 34 (1995) 365.
- [2] K.J. An, D.H. Lee, J.B. Yoo, J. Lee, G.Y. Yeom, J. Vac. Sci. Technol., A 17 (1999) 1483.
- [3] M.V. Bazylenko, M. Gross, M. Faith, Appl. Phys. Lett. 69 (1996) 2178.
- [4] M.V. Bazylenko, M. Gross, J. Vac. Sci. Technol., A 14 (1996) 2994.
- [5] B. Kim, K.H. Pkwon, S.H. Park, J. Vac. Sci. Technol., A 17 (1999) 2593.
- [6] I. Popova, V. Zhukov, J.T. Yates, J.G. Chen, J. Appl. Phys. 86 (1999) 7156.
- [7] D. Klyachko, P. Rowntree, L. Sanche, Surf. Sci. 272 (1996) 385.
- [8] T. Do, N.S. McIntyre, Surf. Sci. 440 (1999) 438.
- [9] B.G. Park, J.Y. Bae, T.D. Lee, J. Appl. Phys. 91 (2002) 8789.
- [10] N. Cabrera, N.F. Mott, Rep. Prog. Phys. 12 (1949) 163.
- [11] A. Quade, H. Wulff, H. Steffen, T.M. Tun, R. Hippler, Thin Solid Films 377–388 (2000) 626.
- [12] A.E.T. Kuiper, M.F. Gillies, V. Kottler, G.W. Hooft, J. Appl. Phys. 89 (2001) 1965.
- [13] W.T. Li, D.A.P. Bulla, C. Charles, R. Boswell, J. Love, B. Luther-Davies, J. Vac. Sci. Technol., A 21 (2003) 792.
- [14] W.T. Li, D.R. McKenzie, W.D. McFall, Q.C. Zhang, W. Wisniewski, Solid-State Electron. 44 (2000) 1557.
- [15] A. Herrick, A.J. Perry, R. Boswell, J. Vac. Sci. Technol., A 21 (2003) 955.
- [16] A.J. Perry, D. Vender, R. Boswell, J. Vac. Sci. Technol., B 9 (1991) 310.
- [17] L.I. Maissel, Handbook of Thin Film Technology, McGrawHill Book Company, 1970.